



Climate variability induced drought across the coastal fringes of the Mekong Delta, Vietnam

T. T. T. NGUYEN, P. H. Y. HOANG and T. A. DANG*

Geography Department, College of Education, Vinh University, Nghe An, Vietnam-4300

**University of Science,*

Vietnam National University-Ho Chi Minh City, Vietnam-70000

(Received 19 February 2022, Accepted 27 April 2022)

e mails : *dtan@hcmus.edu.vn; thanhntt@vinhuni.edu.vn; hoangphanhaiyen@vinhuni.edu.vn

सार – भूमंडलीय ऊष्णन की वजह से वर्षा की लगातार कमी के कारण मेकांग डेल्टा (सीएफएमडी) के तटीय किनारे चरम सूखे की घटनाओं का सामना कर रहे हैं। यह शोध सीएफएमडी में सूखे का व्यापक आकलन करने के साथ-साथ पिछले चार दशकों में इसकी बदलती प्रवृत्ति का पता लगाने के लिए किया गया है।

इस शोध को लागू करने के लिए, मानकीकृत वर्षा सूचकांक (एसपीआई) को 1975-2019 की अवधि के दौरान 24 प्रेक्षण स्टेशनों से प्राप्त वर्षा डेटा अनुक्रमों के आधार पर सूखे के लक्षणों को परिभाषित करने के लिए लागू किया गया है, जबकि मान-केंडल परीक्षण और सेन के ढलान अनुमानक को लागू करके सूखे की बदलती प्रवृत्ति का पता चला। पीयरसन उत्पाद-क्षण सहसंबंध (आर) और कप्पा परीक्षण (के) सांख्यिकीय विधियों के माध्यम से वर्षा असंगति सूचकांक (आरएआई) के साथ तुलना करके एसपीआई के प्रदर्शन का मूल्यांकन किया गया। सूखे के अनुकरण के लिए उच्च सहसंबंध मूल्यों (जैसे, आर 0.812 और के 0.283) द्वारा एसपीआई के अच्छे निष्पादन की पुष्टि की गई।

परिणामों ने बताया कि पूरे अध्ययन क्षेत्र में मध्यम से लेकर चरम तक सूखे की स्थिति की अनेक घटनाएँ दर्ज की गईं। SPI6- और SPI12- दोनों महीनों में सूखे के समय के माप में सूखे की स्थिति में एक महत्वपूर्ण ऊर्ध्वमुखी प्रवृत्ति दर्ज की गई। सूखे की महत्वपूर्ण ऊर्ध्वमुखी प्रवृत्ति वर्षा में महत्वपूर्ण गिरावट का प्रमाण है, जिसमें मुख्य घटना अध्ययन क्षेत्र के पश्चिमी किनारे पर केंद्रित है। सामान्य तौर पर, अन्य स्थानों की तुलना में क्षेत्र के पश्चिमी किनारे पर सूखा अधिक बार और अधिक प्रचण्ड होता है।

ABSTRACT. The coastal fringes of the Mekong Delta (CFMD) have been suffered extreme drought events because of a persistent deficiency of rainfall in the context of global warming. This research is conducted to comprehensively assess drought across the CFMD as well as to detect its changing trend over the past four decades.

To implement this research, the Standardized Precipitation Index (SPI) is applied to define drought features based on rainfall data sequences obtained from 24 observation stations during the period 1975-2019 while the changing trends in drought were detected applying the Mann-Kendall test and Sen's slope estimator. The performance of SPI was appraised by comparison with Rainfall Anomaly Index (RAI) through Pearson Product-Moment Correlation (r) and Kappa test (k) statistical methods. The high correlation values (*e.g.*, $r \geq 0.812$ and $k \geq 0.283$) were confirmed the good performance of the SPI for drought simulation.

The results pointed out that the appearance of multiple drought events ranging from moderate to extreme was recorded over the entire study area. A significant upward trend was recorded for drought appearance on both the SPI6- and SPI12-month drought time scales. A significant upward trend of drought is proof of a significant decline in rainfall, with the main occurrence focusing on the western fringe of the study area. In general, drought is more frequent and severe in the western fringe of the area as compared to other locations.

Key words – Coastal fringes, SPI, RAI, Kappa test, Mann-Kendall test.

1. Introduction

Rainfall is rated as one of the key meteorological parameters, dominating many aspects of human life,

especially the agriculture sector (Becker *et al.*, 2021). The long-term deficiency of rainfall has caused drought, resulting in large global agricultural damage (Asadi *et al.*, 2015). Studies on the effects of drought on agricultural

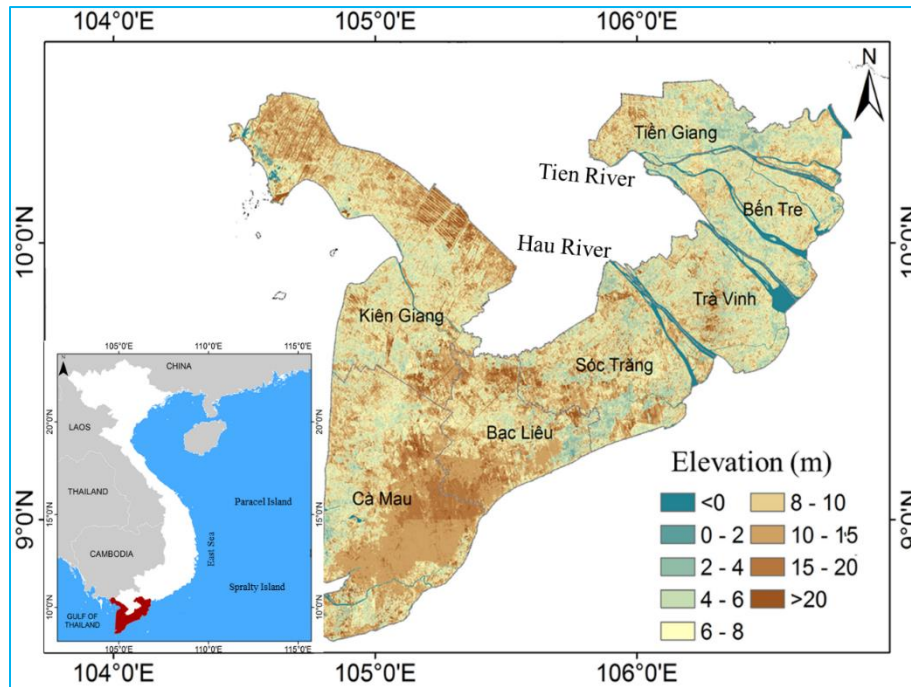
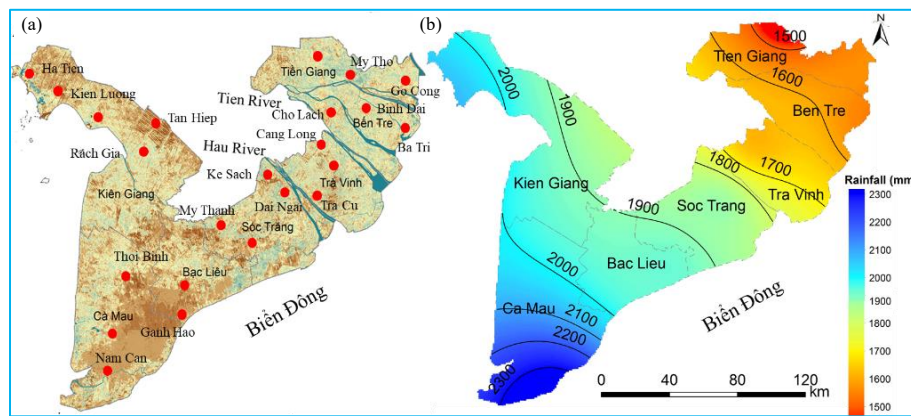


Fig. 1. Topography and elevation map of the study area



Figs. 2(a&b). Spatial distribution of (a) rainfall observation stations and (b) annual mean rainfall at all observation stations across the study area for the period 1975-2019

activities resulted that drought has caused millions of economic losses each year (Miyan, 2015). The coastal fringes of the Mekong Delta (CFMD) are situated in the region of southwestern Vietnam where the agriculture-dominated activity (Lee and Dang, 2019). According to Lee and Dang (2019), the decline in rainfall leads to drought and scarce irrigation water in the Mekong Delta. Especially, the decline in rainfall caused an extreme drought event with Vietnam's economic damage of over \$400 million (CCAFS, 2021). Notably, in the stage 2014-2016, the worst drought event in history at that time happened over the entire CFMD, resulting in 140,000 ha of rice paddies severely affecting crop yield (Dang, 2022).

Numerous studies on the assessment of droughts have been widely deployed in other regions of the world (Abeysingha and Rajapaksha, 2020; Achour *et al.*, 2020). For example, studies on the spatio-temporal drought distribution in the state of Minas Gerais in Brazil by Juliani and Okawa (2017), in the Sarawak River Basin, Malaysia by Bong and Richard (2019), in Sichuan Province, China by Liu *et al.* (2021) and in Vietnam by Dang (2021).

In Vietnam, numerous regions have witnessed repeating and prolonged droughts of an average of about 3-4 years and accompanied by severe water scarcity,

TABLE 1
Basic statistical features of rainfall at 24 observation stations across the study area

| Station | Latitude (°N) | Longitude (°E) | Min. Rainfall(mm) | Max. Rainfall(mm) | Avg. Rainfall(mm) | SD(mm) | CV | Period |
|------------|---------------|----------------|-------------------|-------------------|-------------------|--------|-------|-----------|
| Rach Gia | 10°00' | 105°04' | 1534.5 | 2786.8 | 2110.7 | 329.8 | 86.7 | 1975-2019 |
| Ha Tien | 10°22' | 105°30' | 1487.9 | 3646.7 | 2677.3 | 624.2 | 219.7 | 1981-2019 |
| Kien Luong | 10°18' | 104°38' | 1554.9 | 2614.8 | 2686.4 | 564.2 | 238.9 | 1986-2019 |
| Tan Hiep | 10°30' | 105°09' | 1367.5 | 3986.4 | 2830.4 | 768.4 | 245.9 | 1982-2019 |
| Ca Mau | 09°11' | 105°09' | 1912.4 | 3549.4 | 2386.1 | 299.4 | 82.6 | 1975-2019 |
| Nam Can | 08°45' | 105°42' | 1789.2 | 3674.8 | 2339.8 | 276.9 | 79.5 | 1984-2019 |
| Thoi Binh | 09°21' | 105°05' | 1682.7 | 3546.5 | 1987.4 | 259.3 | 86.9 | 1984-2019 |
| Bac Lieu | 09°17' | 105°43' | 1376.3 | 2817.8 | 1945.8 | 278.7 | 91.5 | 1984-2019 |
| Ganh Hao | 09°02' | 105°25' | 1297.2 | 1989.5 | 1885.7 | 269.7 | 105.9 | 1984-2019 |
| Soc Trang | 09°36' | 105°58' | 1352.8 | 2754.2 | 1891.3 | 298.4 | 87.9 | 1984-2019 |
| Dai Ngai | 09°44' | 106°04' | 538.1 | 2825.9 | 1898.9 | 353.9 | 145.3 | 1982-2019 |
| My Thanh | 09°26' | 105°59' | 701.5 | 2305.4 | 1598.4 | 347.2 | 189.7 | 1982-2019 |
| Ke Sach | 09°48' | 105°55' | 1512.1 | 3865.3 | 1946.2 | 297.8 | 194.2 | 1983-2019 |
| Cang Long | 09°59' | 106°12' | 1200.1 | 2041.4 | 1635.7 | 219.7 | 91.2 | 1987-2019 |
| Tra Cu | 09°47' | 106°10' | 1245.3 | 1865.9 | 1547.6 | 221.5 | 112.9 | 1982-2019 |
| Tra Vinh | 09°54' | 106°25' | 911.7 | 1956.4 | 1456.8 | 233.7 | 156.1 | 1980-2019 |
| Ba Tri | 10°03' | 106°36' | 1133.2 | 2238.2 | 1536.4 | 257.9 | 92.7 | 1981-2019 |
| Cho Lach | 10°14' | 106°10' | 1212.7 | 1799.8 | 1456.9 | 125.8 | 99.6 | 1983-2019 |
| Binh Dai | 10°11' | 106°41' | 1239.8 | 2005.9 | 1652.8 | 127.4 | 98.2 | 1983-2019 |
| Ben Trai | 10°02' | 106°19' | 1107.4 | 1829.2 | 1452.8 | 192.5 | 106.7 | 1980-2019 |
| My Tho | 10°21' | 106°23' | 816.4 | 1893.6 | 1445.9 | 246.8 | 79.5 | 1982-2019 |
| Go, Cong | 10°18' | 106°42' | 1067.8 | 1985.4 | 1423.4 | 224.2 | 113.5 | 1983-2019 |
| Long Dinh | 10°23' | 106°15' | 1257.8 | 1574.6 | 1344.8 | 184.5 | 119.6 | 1984-2019 |
| Vam Kenh | 10°16' | 106°44' | 1358.3 | 1798.3 | 1497.5 | 168.9 | 98.7 | 1984-2019 |

Min- minimum; Max- maximum; Avg- average; SD-standard deviation; CV- coefficient of variation

resulting in socio-economic development. Droughts are of major concern in Vietnam because much of the sub region is highly drought-prone experiencing drought very frequently but detailed research regarding drought in the sub-region is still lacking (Lee and Dang, 2019). Therefore, the aims of this study are (i) a comprehensive assessment of drought across the CFMD based on the SPI and (ii) to detect drought trends by applying the Mann-Kendall test and Sen slope estimator.

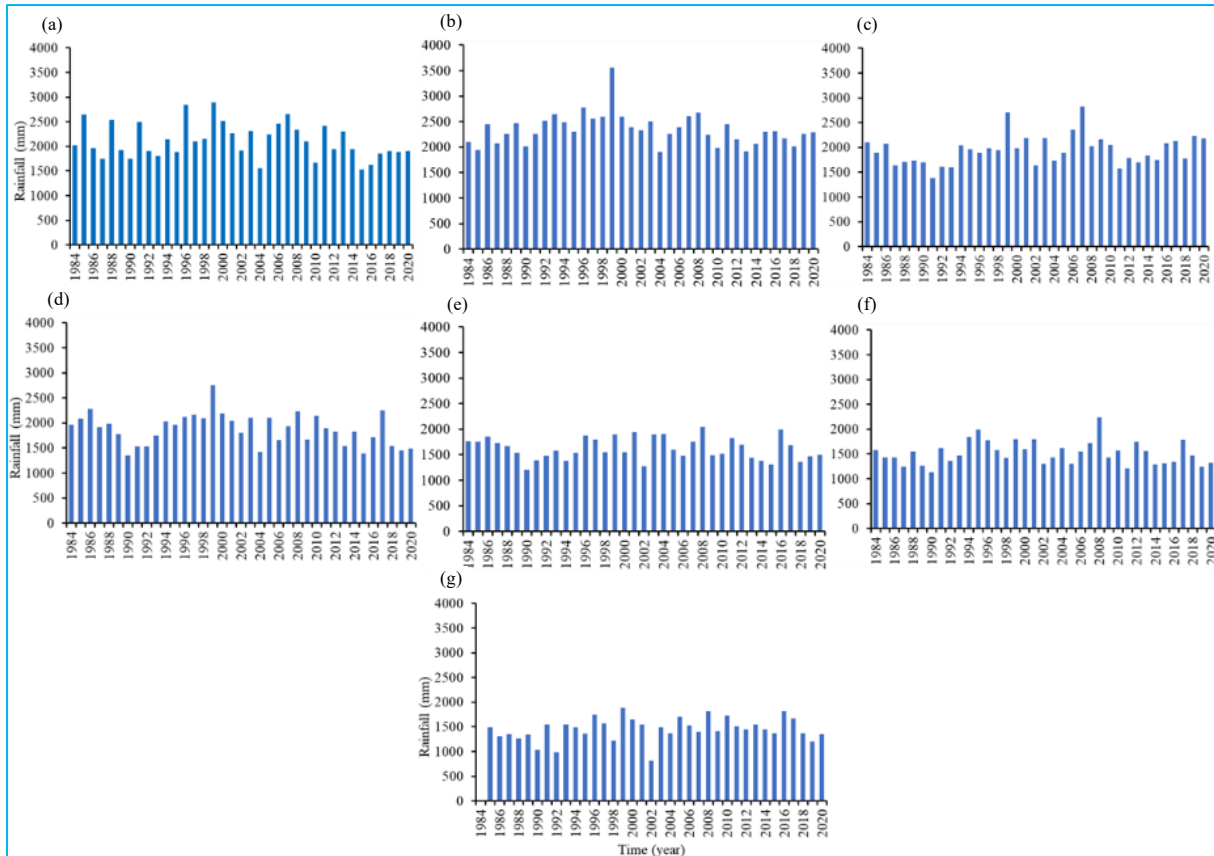
2. Materials and method

2.1. Study area

The coastal fringes surrounded the entire Mekong Delta includes Kien Giang, Ca Mau, Bac Lieu, Soc Trang,

Tra Vinh, Ben Tre and Tien Giang province, stretching from the latitudes 08°33'0" N -10°25'13.04" N and longitudes of 104°26'40" E - 106°30'0" E (Fig. 1) with a total land area approximately 28.422 km² in which agricultural production and aquaculture dominate compared to prevail over other fields in the area (Dang *et al.*, 2021; Vu *et al.*, 2017).

The area signifies to lower from north to south and from east to west with the altitude in ranges from 0.5 to 3.0 m.a.s.l. Tien River and Hau River are the two main sources of irrigation water, the coastal lowland fringes have expanses of flatlands [Fig. 2(a)] where the two main rivers flow from the upstream to the coastal lowland fringes in the southern part (Lee and Dang, 2019). The CFMD lied in the tropical monsoon climate zone with the



Figs. 3(a-g). Temporal distribution of annual mean rainfall at seven representative observation stations includes (a) Rach Gia, (b) Ca Mau, (c) Bac Lieu, (d) Soc Trang, (e) Cang Long, (f) Ba Tri and (g) My Tho during the period 1975-2019

mean annual temperature ranges from 26.3 to 29.1°C and the mean annual rainfall ranges from 1334.8 to 2830.4 mm (Table 1) of which 89% of the annual rainfall occurs during the rainy season from May to November. Specifically, the eastern fringe gets the high annual rainfall up to 2400 mm while the western fringe only picks up the low annual rainfall of approximately 1600 mm [Table 1; Fig. 2(b)].

2.2. Rainfall data collection

To implement this work, rainfall data sequences at 24 observation stations were obtained from the National Center for Hydrometeorological Forecasting (NCHF) of Vietnam. Daily rainfall data at 24 stations recorded during the period 1975-2019 with the location of the stations is shown in Fig. 2(a) and the spatial distribution of rainfall at 24 rainfall observation stations is illustrated in Fig. 2(b). To warrant the reliability of the statistical analysis, rainfall data sequences at any station do not miss over 10 per cent. In addition, the rainfall data sequences at all observation stations were considered for heterogeneity, randomness and correlation.

Thiessen polygon method of defining a real significance to point rainfall values was applied to interpolate the rainfall distribution based on the ArcGIS software. Fig. 2(b) annotates annual rainfall distribution across the study area, it's easy to find out that the eastern fringe [Figs. 3(a&b)] of the area received less rainfall than the western fringe [Figs. 3(c-g)].

2.3. Standardized Precipitation Index (SPI)

The SPI is progressed by McKee *et al.* (1993) for intending to seek the alteration in the rainfall data sequences for multiple timescales based on the probability distribution of rainfall to support early warning as well as tracking drought events (Khan *et al.*, 2020; Dhurmea *et al.*, 2019). The SPI was applied in the current research due to its effectiveness in drought simulation and detecting its severity through quantitative classifier values (Fung *et al.*, 2020; Hänsel *et al.*, 2016). The SPI values are defined based on the total volume of rainfall for any timescales (*e.g.*, 1, 3, 6, 12, 24 and 48 months), depending on the original targets of the research. The SPI explores the changes in the long-term rainfall sequences based on

fitting a Gamma distribution function to a long-term rainfall sequence (McKee *et al.*, 1993). Then, the SPI values were obtained through the normal standardization function (PDF) (WMO, 2012). The PDF is presented as in Eqn. 1.

$$G(x) = \frac{x^{\alpha-1} e^{-x/\beta}}{\beta^\alpha \Gamma(\alpha)}; (x > 0) \quad (1)$$

where, β and α - the scale and shape parameters

x - the precipitation amount

$\Gamma(\alpha)$ -the Gamma function.

whereby, the cumulative distribution function [$G(x)$] is defined through integrating the PDF as given in Eqn. 2.

$$G(x) = \int_0^x g(x)dx = \int_0^x \frac{x^{\hat{\alpha}-1} e^{-x/\hat{\beta}}}{\hat{\beta}^{\hat{\alpha}} \Gamma(\hat{\alpha})} dx \quad (2)$$

In the Eqn. 2, the $\hat{\alpha}$, $\hat{\beta}$ parameters are defined through Eqn. 3 and Eqn. 4.

$$\hat{\alpha} = \frac{1}{4A} \left(1 + \sqrt{1 + \frac{4A}{3}} \right) \quad (3)$$

$$\hat{\beta} = \frac{\hat{x}}{\hat{\alpha}} \quad (4)$$

A parameter in Eqn.3 is calculated through Eqn. 5.

$$A = \ln(\bar{x}) - \frac{\sum \ln(x)}{n} \quad (5)$$

where, \bar{x} , x and n - sample average value, sample value and number of observed rainfall samples.

Finally, the SPI index is obtained from Eqn. 6.

$$SPI = \psi^{-1}[G(x)] \quad (6)$$

Accordingly, based on the classification of the SPI values provided by McKee *et al.* (1993). Whereby, the location of the area is considered as moderate, severe and extreme dry if the SPI values are negative and reach an intensity from -1.0 to less than -2.0 (Table 2). This implies

TABLE 2

The SPI categories are based on the drought scale classification (WMO, 2012)

| Interval | SPI values |
|----------------|----------------|
| -0.99 to 0.99 | Near normal |
| -1.00 to -1.49 | Moderately dry |
| -1.50 to -1.99 | Severely dry |
| <-2.00 | Extremely dry |

that the rainfall interval has a lower value than its average value (McKee *et al.*, 1993).

Based on the advantages, the SPI has been recognized as a standard index that should be applied for detecting the changes in rainfall related to climate variability (Dang, 2021; Juliani and Okawa, 2017). Furthermore, at the Inter-Regional Workshop on Indices and Early Warning Systems for Drought, World Meteorological Organization (WMO) induced meteorological agencies of member states should use the SPI for tracking as well as monitoring droughts (Bayissa *et al.*, 2018; Hayes *et al.*, 2011). National meteorological agencies of Brazil, Paraguay, Uruguay, Argentina, China and over 80 meteorological agencies of other member states then, have been used the SPI for studying drought in their countries (Liu *et al.*, 2021).

2.4. Mann-Kendall test

The non-parametric statistical method namely Mann-Kendall is applied in the current research to detect monotonic trends in rainfall data sequences. Accordingly, the null hypothesis (H_0) is that the data come from a population with independent realizations and are identically distributed. The alternative hypothesis (H_A) is that the data follow a monotonic trend. The Mann-Kendall test statistic is given as follows:

$$S = \sum_{i=1}^{n-1} \sum_{j=k+1}^n \text{sgn}(x_j - x_k) \quad (7)$$

$$\text{with } \text{sgn}(x_j - x_i) = \begin{cases} 1 & \text{if } (x_j - x_i) > 0 \\ 0 & \text{if } (x_j - x_i) = 0 \\ -1 & \text{if } (x_j - x_i) < 0 \end{cases} \quad (8)$$

The mean of S is $E[S] = 0$ and the variance σ^2 is

$$\sigma^2 = \frac{1}{18} \left[n(n-1)(2n+5) - \sum_{j=1}^p t_j(t_j-1)(2t_j+5) \right] \quad (9)$$

where, p is the number of the tied groups in the data set and t_j is the number of data points in the j^{th} tied group. The statistic S is closely normal distributed accommodated that the following Z-transformation is employed:

$$Z_{MK} = \begin{cases} \frac{S-1}{\sigma} & \text{if } S > 0 \\ 0 & \text{if } S = 0 \\ \frac{S+1}{\sigma} & \text{if } S < 0 \end{cases} \quad (10)$$

The statistic S is closely related to Kendall's τ as defined by Eqn. 11.

$$\tau = \frac{S}{D} \quad (11)$$

where D is defined by Eqn. 12.

$$\sigma^2 = \frac{1}{18} \left[n(n-1)(2n+5) - \sum_{j=1}^p t_j(t_j-1)(2t_j+5) \right] \quad (12)$$

The value of Z_{MK} in Eqn. 10 is considered the Mann-Kendall test that follows a normal distribution with mean 0 and variance 1. The Mann-Kendall value at a specific significance level (α) will respond it's a trend. Where $|Z_{MK}| > Z_{1-\alpha/2}$, the null hypothesis is rejected and a significant trend exists in the time sequences. $Z_{1-\alpha/2}$ is defined from the normal distribution. In this research, the Mann-Kendall test is used to detect the changing trend in the rainfall data sequences at all observation stations with 95% confidence intervals ($\alpha = 0.05$).

2.5. Pearson product-moment correlation

Pearson product-moment correlation (r) is a measure of the strength of the linear relationship between two data variables. R tries to sketch a line of best fit based on two existing data variables and its coefficient points out how far away all these data points are from this line of best fit (Vergni *et al.*, 2021). Commonly, the r -value lies between -1 and +1, a value less/greater than 0 implies a negative/position association while the r -value of 0 implies that there is not any association between two existing data variables (Schober *et al.*, 2018). Pearson product-poment correlation can be calculated by Eqn.13.

TABLE 3

Classification ranges of the k statistic corresponding strength of agreement

| k statistic | Classification ranges |
|-------------|-----------------------|
| <0.00 | Poor |
| 0.00-0.02 | Slight |
| 0.21-0.40 | Fair |
| 0.41-0.60 | Moderate |
| 0.61-0.80 | Substantial |
| 0.81-1.00 | Almost perfect |

$$r = \frac{\sum (x_i - \bar{x})(y_i - \bar{y})}{\sqrt{\sum (x_i - \bar{x})^2 \sum (y_i - \bar{y})^2}} \quad (13)$$

where,

x_i – the value of the x -variable in a sample

\bar{x} – the mean value of the x -variable

y_i – the value of the y -variable in a sample

\bar{y} – the mean value of the y -variable

2.6. Cohen's Kappa test

Cohen's Kappa test is a measure of agreement between two existing data variables. The K test is commonly used to assess the applied agreement between methods. In this research, the Cohen's Kappa test is used to compare the similarity between the SPI and RAI. The Cohen's Kappa test is commonly defined through the coefficient of agreement K, corrected for chance (Schober *et al.*, 2018; Vergni *et al.*, 2021).

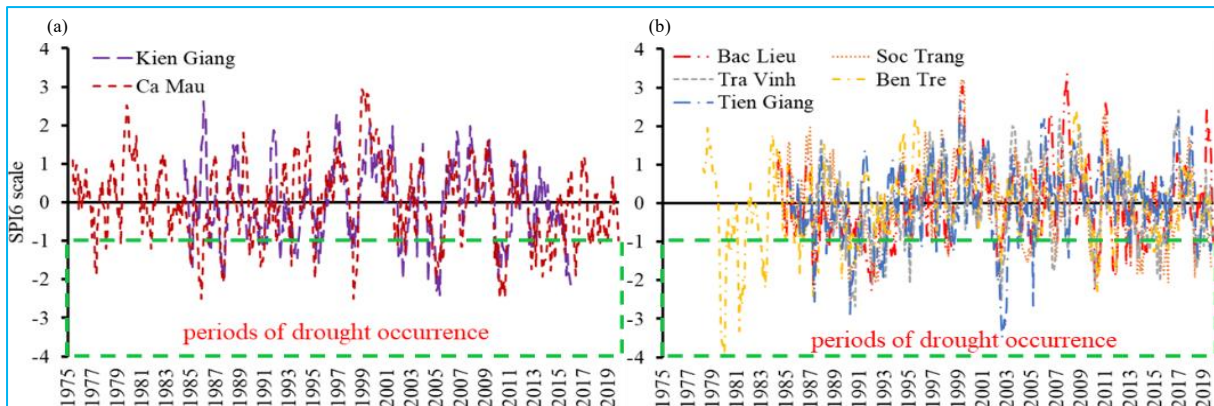
The proportion agreement between two existing data variables X and Y is calculated by:

$$p_0 = \frac{1}{n} \sum_{i=1}^g XY \quad (14)$$

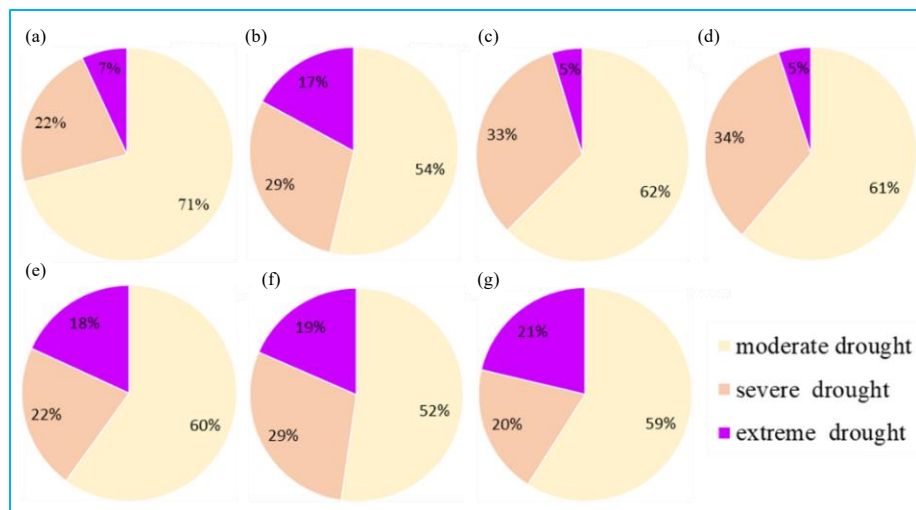
and the expected agreement by chance is defined by Eqn. 15:

$$p_e = \frac{1}{n^2} \sum_{i=1}^g XY \quad (15)$$

where, X is the total for the row and Y is the total for the column.



Figs. 4(a&b). Distribution of the SPI6-month drought timescale at (A) Kien Giang, Ca Mau, and (B) Bac Lieu, Soc Trang, Cang Long, Ba Tri and My Tho station across the study area during the period of 1975-2019



Figs. 5(a-g). Distribution of the SPI12-month drought timescale at (a) Rach Gia, (b) Ca Mau, (c) Bac Lieu, (d) Soc Trang, (e) Cang Long, (f) Ba Tri and (g) My Tho station across the study area during the period of 1975-2019

The K test is defined by Eqn. 16.

$$K = \frac{P_0 - P_e}{1 - P_e} \quad (16)$$

Weighted kappa can be given in Table 3 with ordinal categories.

3. Results and discussion

3.1. Temporal analysis of droughts

According to Khan *et al.* (2020), the change in the short-term rainfall has a close relation to the 3-month drought timescale (SPI3) while the long-term drought timescales (*e.g.*, 9, 12, 18, 24 months or more) are closely

linked to surface water storage. Therefore, rainfall accumulation over long-term scales becomes more important for reservoir storage (McKee *et al.*, 1993). For temporal analysis of droughts based on the SPI for timescales of 3-, 6-, 9- and 12-months was conducted for seven representative observation stations across the study area [Fig. 2(a)] during the period 1975-2019. A detailed analysis of temporal alteration of the drought across the study area is carried out here with the 6 and 12 drought scales (SPI6 and SPI12).

For the analysis of the SPI6-month drought scale time, the western fringe of the study area includes Kien Giang and Ca Mau provinces recorded an average total of 77 drought events with classification from moderate to extreme scales [Figs. 4(a&b)] while the eastern fringe includes Bac Lieu, Soc Trang, Tra Vinh, Ben Tre and

TABLE 4

Characteristics of SPI6-month drought timescale across the study area in the period of 1975-2019

| Station | MD | SD | ED | Risk peak | Duration (month) | Start date | End date |
|----------------|-------------|-------------|------------|--------------|------------------|------------|----------|
| Rach Gia | 51 | 16 | 5 | -2.42 | 9 | 2004-Sep | 2005-May |
| Ca Mau | 44 | 24 | 14 | -2.50 | 6 | 1985-Aug | 1986-Jan |
| Bac Lieu | 40 | 21 | 3 | -2.27 | 11 | 1991-Jun | 1992-Apr |
| Soc Trang | 49 | 27 | 4 | -2.65 | 13 | 1990-Apr | 1991-Apr |
| Cang Long | 33 | 12 | 10 | -2.68 | 10 | 1990-Feb | 1990-Dec |
| Ba Tri | 34 | 19 | 12 | -2.41 | 6 | 1987-May | 1987-Oct |
| My Tho | 36 | 12 | 13 | -3.49 | 15 | 2002-Feb | 2003-Apr |
| Average | 41.0 | 18.7 | 8.7 | -2.63 | 10 | - | - |

MD - moderate drought; S - severe drought; E - extreme drought

TABLE 5

Characteristics of SPI12 drought timescale across the area in the period of 1975-2019

| Station | MD | SD | ED | Risk peak | Duration (month) | Start date | End date |
|----------------|-------------|-------------|------------|--------------|------------------|------------|----------|
| Rach Gia | 47 | 19 | 3 | -2.04 | 12 | 2010-Mar | 2011-Feb |
| Soc Trang | 48 | 29 | 6 | -2.21 | 37 | 1990-May | 1993-May |
| My Tho | 14 | 18 | 17 | -3.57 | 14 | 2002-Jun | 2003-Jul |
| Bac Lieu | 54 | 3 | 5 | -2.17 | 35 | 1991-Jun | 1994-Apr |
| Ba Tri | 39 | 23 | 13 | -3.12 | 32 | 1979-Oct | 1982-May |
| Cang Long | 49 | 20 | 7 | -3.06 | 14 | 1990-May | 1991-Jun |
| Ca Mau | 46 | 33 | 5 | -2.62 | 26 | 2013-Mar | 2015-Apr |
| Average | 43.3 | 21.6 | 8.9 | -2.95 | 31.2 | - | - |

MD - moderate drought; S - severe drought; E - extreme drought

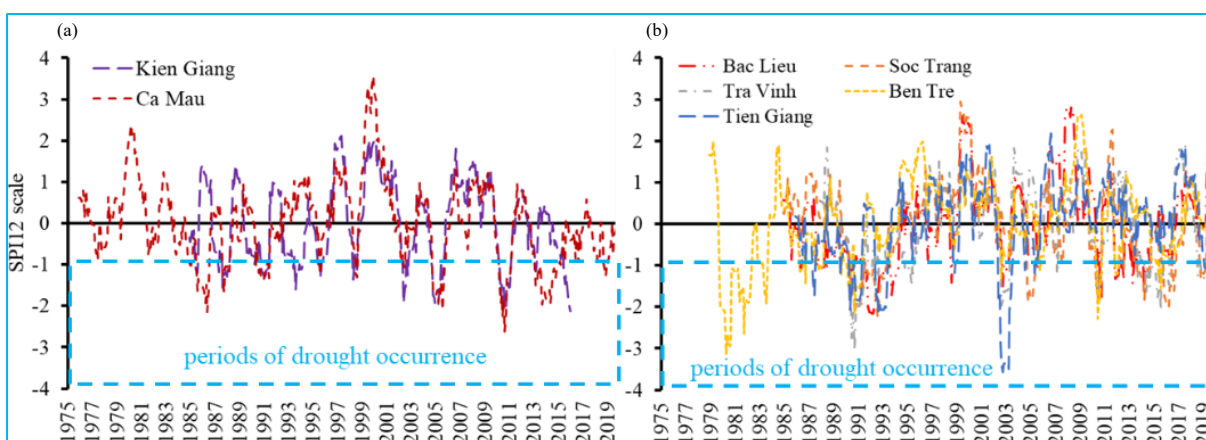
Tien Giang provinces appeared an average total of 65 drought events [Figs. 4(c-g)].

A drought event with risk peak intensity up to 3.49 was recorded at My Tho station (located in the eastern fringe of the study area) and lasted for 15 months from 2002-Feb to 2003-Apr [Fig. 5(b)] while drought events with peak intensities varying from 2.27 to 2.68 associated with durations of 10 months occurred in the western fringe [Fig. 5(a)]

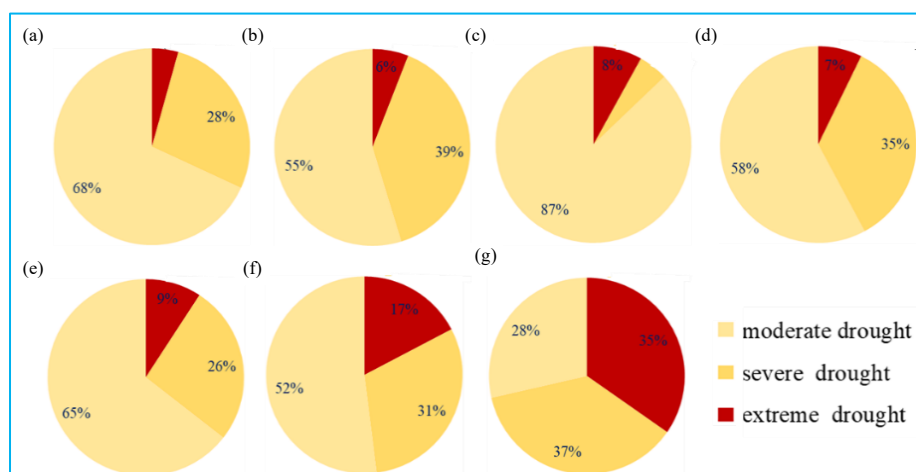
Generally, in the period of 1975-2019, the western fringe of the study area appeared more severe, moderate and extreme drought than the eastern fringe. Specifically, an average total of 47.5, 20.0 and 9.5 severe, moderate and extreme drought events were recorded in the western fringe while the corresponding values at the eastern fringe recorded 38.4, 18.0 and 8.4 respectively (Table 4).

For the analysis of the SPI12-month drought scale time, during the period 1975-2019, the area recorded an average total of 43.3, 21.6 and 8.9 moderate, severe and extreme drought months (Table 5). The western fringe only appeared an average total of 5.0% extreme drought events [Figs. 6(a&b)] while the eastern fringe recorded an average total of 15.2% extreme drought events [Fig. 6(a)]. Specifically, Tien Giang station appeared up to 35.0% of extreme drought events [Fig. 6(b)]. It implies that Tien Giang province is facing a high risk of drought, leading to a lack of irrigation water for agricultural production, especially in the dry season.

The longest duration of moderate drought event continuously lasted up to 80 months (from 1987-Sep to 1994-April) at Bac Lieu station (an eastern fringe of the study area) and the maximum intensity recorded up to 2.17 in 1992 [Fig. 7(b)]. The longest duration of severe



Figs. 6(a&b). Distribution of the SPI12-month drought timescale at (a) Rach Gia, Ca Mau and (b) Bac Lieu, Soc Trang, Cang Long, Ba Tri and My Tho station across the study area during the period of 1975-2019



Figs. 7(a-g). Results of the SPI12 drought timescale at stations belonging to (a) western fringe and (b) eastern fringe during the period 1975 to 2019

drought events recorded 33 months from 2013-March to 2015-April at Ca Mau station (a western fringe of the study area) and the maximum intensity detected 1.96 in 2013 [Fig. 7(a)]. While the longest duration of extreme drought events only stretched 17 months at My Tho station with the risk maximum intensity discovered up to 3.57 (Table 5).

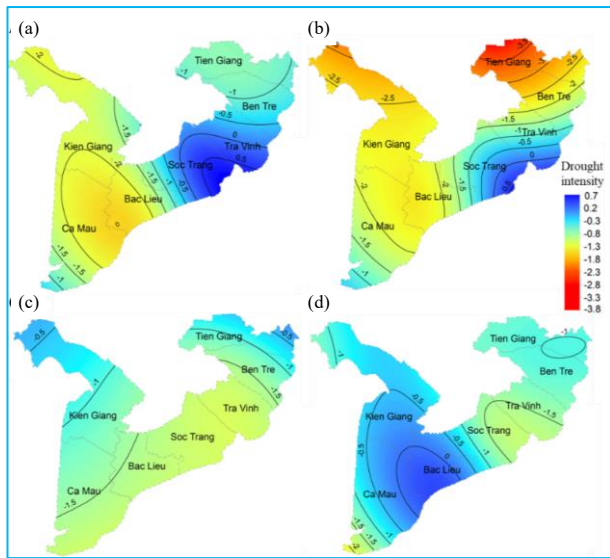
3.2. Spatial analysis of droughts

The spatial distribution of the SPI12-month drought timescale for seven representative observation stations across the study area is presented in Fig. 8. During the studied period (1975-2019), the four typical drought events were swept in the entire study area (Table 6). In 1998, near-normal weather to severe droughts occurred in the entire study area. Specifically, near-normal weather to

TABLE 6

Spatial distribution of historical drought events that occurred across the study area from 1975 to 2019

| S. No. | Station | Maximum intensity | | | |
|--------|-----------|-------------------|-------|-------|-------|
| | | 1998 | 2002 | 2014 | 2019 |
| 1. | Rach Gia | -1.57 | -1.94 | -0.57 | -1.49 |
| 2. | Ca Mau | -1.52 | -1.07 | -1.93 | -1.29 |
| 3. | Bac Lieu | -1.42 | -1.50 | -1.72 | -0.17 |
| 4. | Soc Trang | 0.35 | -0.46 | -1.82 | -1.54 |
| 5. | Cang Long | -0.59 | -1.97 | -1.79 | -1.28 |
| 6. | Ba Tri | -0.63 | -1.31 | -0.87 | -1.09 |
| 7. | My Tho | -1.19 | -3.57 | -0.35 | -1.10 |



Figs. 8(a-d). Spatial distribution of typical drought events based on the SPI12-month scaletime in (a) 1998, (b) 2002, (c) 2014 and (d) 2019 across the entire study area

moderate droughts intervened in the eastern fringe of the study area with the peak values ranging from 0.35 to -1.42 while the western fringe recorded severe drought with the risk peak up to -1.57 in 1998 [Fig. 8(a)].

In 2002, multiple drought scales from near normal weather to extreme drought appeared in almost the whole area. Specifically, moderate to severe droughts with the SPI12 value -1.07 and -1.94, respectively were defined in the western fringe while near-normal weather (SPI = -0.46) to extreme droughts (SPI = -3.57) were recorded in the eastern fringe of the study area [Fig. 8(b)].

For the 2014 drought event, near-normal weather to severe droughts swept over the entire study area and the whole study area did not record any severe drought events [Fig. 8(c)]. In January 2019, the results of SPI12 month drought scale time indicated near-normal weather to moderate droughts. Specifically, the eastern fringe of the study area occurred near-normal weather to moderate drought while the western fringe only detected moderate drought [Fig. 7(d)]. Similar results were also reported by Lee and Dang (2019) that the Mekong Delta experienced the four typical drought stages including 1996-1998, 2002-2004, 2014-2016 and 2018-2019 and drought severity levels ranged from near normal weather to extreme drought.

3.3. Trend analysis of droughts characteristics

Change trends of drought across the study area are analyzed applying the Mann-Kendall test and Sen's slope

TABLE 7

Change trends of drought across the study area in the period 1975-2019

| No. | Station | Man-Kendall | | Sen's slope | Trend |
|-----|-----------|-------------|---------|-------------|----------|
| | | Z_D | p-value | β | |
| 1. | Rach Gia | 1.963 | 0.347 | 5.482 | Upward |
| 2. | Ca Mau | 1.979 | 0.218 | 4.883 | Upward |
| 3. | Bac Lieu | -0.967 | 0.841 | -3.794 | Downward |
| 4. | Soc Trang | 1.994 | 0.216 | 4.864 | Upward |
| 5. | Cang Long | 0.045 | 0.796 | 0.096 | Upward |
| 6. | Ba Tri | -0.946 | 0.492 | -2.937 | Downward |
| 7. | My Tho | -0.951 | 0.573 | -3.468 | Downward |

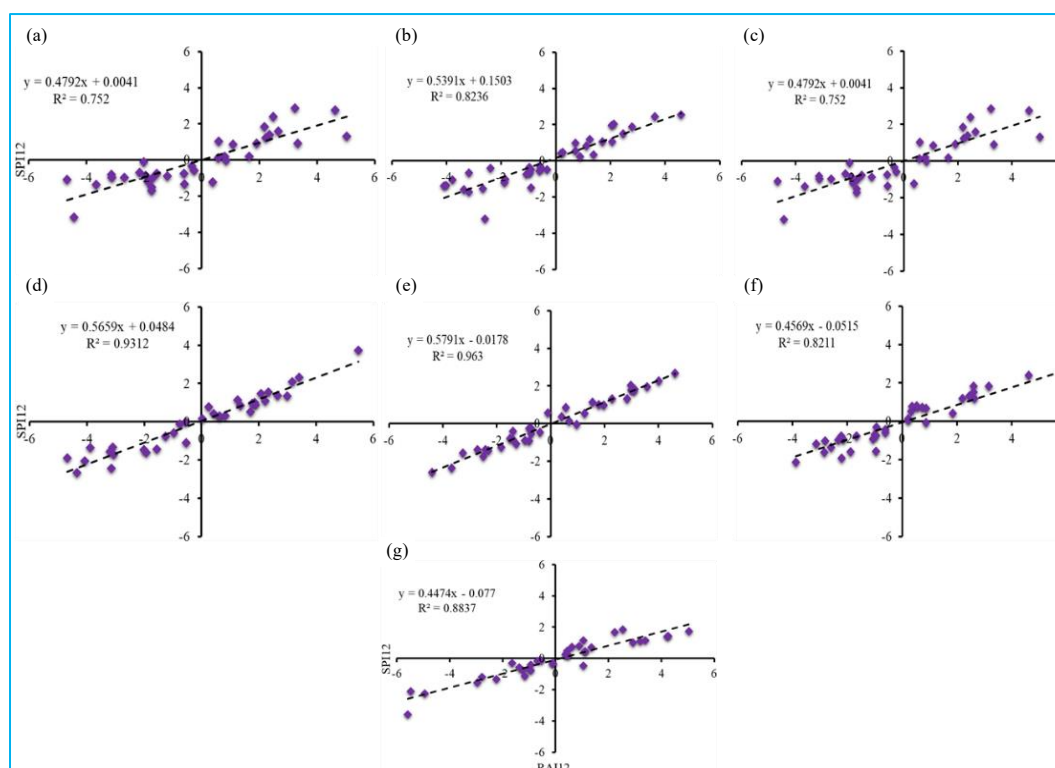
estimator with 95% confidence intervals ($\alpha = 0.05$). According to the finding results, a light upward trend in drought ($Z_D = 0.045-1.394$ and $\beta = 0.09-1.864$) are recorded at Cang Long and Soc Trang stations while a significant upward trend with the Z_D varied from 1.963 to 1.994 and the β value varied from 4.864 to 5.482, respectively are found at Rach Gia and Ca Mau stations (the western fringe of the study area) (Table 7).

Contrary, a slight downward trend is found at Bac Lieu, Ba Tri and My Tho stations (the eastern fringe of the study area) with the Z_D varied from -0.967 to -0.946, respectively and the β values ranging from -3.794 to -2.937, respectively. Similar findings have been stated by Lee and Dang, (2019). Their results indicated a downward trend in rainfall leading to drought in the western coastal areas of the Mekong Delta in the period 1984-2015.

3.4. Comparison of SPI results with RAI

The performance of the SPI for the detection of drought events across the study area was appraised by comparing it with RAI (Table 8). Correlation between SPI and RAI for 3, 6, 9 and 12-month timescales at all the rainfall observation stations across the entire study area are rated based on Pearson's correlation coefficient (r) and Cohen's Kappa (k). Specifically, the obtained values of the r correlation coefficient ranged from 0.812 to 0.945 for SPI3 and RAI3 month drought scale time while the higher values varied from 0.854 to 0.981 were also obtained for the 6-, 9- and 12-month drought timescales between SPI and RAI [Figs. 9(a-g)].

Moreover, to assess the strength of agreement between the SPI and RAI, the Cohen's Kappa (k) test was



Figs. 9(a-g). Correlation between SPI12 and RAI12-month drought timescales at seven representative observation stations (a) Rach Gia, (b) Ca Mau, (c) Bac Lieu, (d) Soc Trang, (e) Cang Long, (f) Ba Tri and (g) My Tho during the period 1975-2019

TABLE 8

Comparison between SPI and RAI for 3, 6, 9 and 12-month drought timescales across the study area during the period 1975-2019

| Stations | Correlation between SPI3 and RAI3 | | Correlation between SPI6 and RAI6 | | Correlation between SPI9 and RAI9 | | Correlation between SPI12 and RAI12 | |
|-----------|-----------------------------------|-------|-----------------------------------|-------|-----------------------------------|-------|-------------------------------------|-------|
| | r | k | r | k | r | k | r | k |
| Rach Gia | 0.812 | 0.283 | 0.854 | 0.289 | 0.867 | 0.299 | 0.867 | 0.318 |
| Ca Mau | 0.876 | 0.285 | 0.915 | 0.288 | 0.921 | 0.315 | 0.917 | 0.317 |
| Bac Lieu | 0.890 | 0.297 | 0.912 | 0.297 | 0.932 | 0.309 | 0.900 | 0.326 |
| Soc Trang | 0.913 | 0.314 | 0.953 | 0.334 | 0.965 | 0.339 | 0.964 | 0.343 |
| Cang Long | 0.945 | 0.345 | 0.978 | 0.355 | 0.946 | 0.365 | 0.981 | 0.372 |
| Ba Tri | 0.852 | 0.293 | 0.894 | 0.315 | 0.917 | 0.317 | 0.906 | 0.322 |
| My Tho | 0.876 | 0.296 | 0.913 | 0.327 | 0.909 | 0.326 | 0.914 | 0.318 |

r-Pearson's correlation; k - Cohen's Kappa test

also applied. Specifically, the results pointed out that the values of k between SPI3 and RAI3 month drought scale time ranged from 0.283 to 0.345, which implies a fair agreement between the SPI3 and RAI3. Similarly, a good agreement between SPI and RAI for the 6-, 9- and 12-month drought timescales were also obtained with the values of k varying from 0.289 to 0.372 (Table 8).

4. Conclusions

(i) A comprehensive study of drought characteristics in the period 1975-2019 across the coastal fringes of the Mekong Delta was conducted based on the Standardized Precipitation Index and the non-parametric statistical methods at the 95% significance level.

(ii) Based on the findings, the appearance of multiple drought events ranging from moderate to extreme was recorded over the entire area during the study period of 1975-2019. Research also indicated that increasing trend in the severity of drought recorded in the western fringe of the study area.

(iii) A record drought trend is proof of a significant decline in rainfall, with the main occurrence focusing on the western fringe of the study area. In general, drought is more frequent and severe in the western fringe of the area as compared to other locations.

(iv) The analyzed results of drought based on the Standardized Precipitation Index are useful for planning the efficient use of water resources and agricultural production.

Disclaimer: The contents and views expressed in this study are the views of the authors and do not necessarily reflect the views of the organizations they belong to.

References

- Abeysingha, N. and Rajapaksha, U., 2020, "SPI-based spatiotemporal drought over Sri Lanka", *Advances in Meteorology*, **2020**, 1-10.
- Achour, K., Meddi, M., Zeroual, A., Bouabdelli, S., Maccioni, P. and Moramarco, T., 2020, "Spatio-temporal analysis and forecasting of drought in the plains of northwestern Algeria using the standardized precipitation index", *Journal of Earth System Science*, **129**, 1-12.
- Asadi, Z. M. A., Sivakumar, B. and Sharma, A., 2015, "Droughts in a warming climate: a global assessment of SPI and RDI", *Journal of Hydrology*, **526**, 183-195.
- Becker, C. C., Streck, N. A., Schwab, N. T., Uhlmann, L. O., Tomiozzo, R. and Ferraz, S. E. T., 2021, "Climate risk zoning for gladiolus production under three climate change scenarios", *Revista Brasileira de Engenharia Agrícola e Ambiental*, **25**, 297-304.
- Bong, C. H. J. and Richard, J., 2019, "Drought and climate change assessment using standardized precipitation index (SPI) for Sarawak River Basin", *Journal of Water and Climate Change*, **11**, 956-965.
- CCAFS- Climate Change, Agriculture and Food Security Southeast Asia Complete With Resounding Success and Minister's Award for Valuable Contribution for Vietnam's Agriculture Development: Hanoi, Vietnam, 2021.
- Dang, T. A., 2021, "Grain yield optimisation in the Plain of Reeds in the context of climate variability", *Revista Brasileira de Engenharia Agrícola e Ambiental*, **25**, 591-596.
- Dang, T. A., Nguyen, V. H. and Mai, P. N., 2021, "Utilizing rainfed supply and irrigation as a climate variability adaptation solution for coastal lowland areas in Vietnam", *Agr. Nat. Resour.*, **55**, 485-495.
- Dhurmea, K. R., Boojhawon, R. and Rughooputh, S. D. D. V., 2019, "A drought climatology for Mauritius using the standardized precipitation index", *Hydrological Sciences Journal*, **64**, 227-240.
- Fung, K. F., Huang, Y. F. and Koo, C. H., 2020, "Assessing drought conditions through temporal pattern, spatial characteristic and operational accuracy indicated by SPI and SPEI : Case analysis for Peninsular Malaysia", *Nat. Hazards*, **103**, 2071-2101.
- Hänsel, S., Schucknecht, A. and Matschullat, J., 2016, "The modified Rainfall Anomaly Index (mRAI) - is this an alternative to the Standardised Precipitation Index (SPI) in evaluating future extreme precipitation characteristics?", *Theor. Appl. Climatol.*, **123**, 827-844.
- Hayes, M., Svoboda, M., Wall, N. and Widhalm, M., 2011, "The Lincoln declaration on drought indices: universal meteorological drought index recommended", *Bulletin of the American Meteorological Society*, **92**, 485-488.
- Juliani, B. H. T. and Okawa, C. M. P., 2017, "Application of a Standardized Precipitation Index for meteorological drought analysis of the semi-arid climate influence in Minas Gerais, Brazil", *Hydrology*, **4**, 2-14.
- Khan, M. I., Zhu, X., Arshad, M., Zaman, M., Niaz, Y., Ullah, I., Anjum, M. N. and Uzair, M., 2020, "Assessment of spatiotemporal characteristics of agro-meteorological drought events based on comparing Standardized Soil Moisture Index, Standardized Precipitation Index and Multivariate Standardized Drought Index", *Journal of Water and Climate Change*, **11**, 1-17.
- Lee, S. K. and Dang, T. A., 2019, "Spatiotemporal variations in meteorology drought over the Mekong River Delta of Vietnam in the recent decades", *Paddy and Water Environment*, **17**, 35-44.
- Liu, C., Yang, C., Yang, Q. and Wang, J., 2021, "Spatiotemporal drought analysis by the standardized precipitation index (SPI) and standardized precipitation evapotranspiration index (SPEI) in Sichuan Province, China", *Scientific Reports*, **11**, 1-14.
- McKee, T. B., Doesken, N. J. and Kleist, J., 1993, "The relationship of drought frequency and duration to time scales", In : Proceedings of the 8th Conference on Applied Climatology, Anaheim, CA, USA, 17-22 January 1993.
- Miyan, M. A., 2015, "Droughts in Asian least developed countries; vulnerability and sustainability", *Weather and Climate Extremes*, **7**, 8-23.
- Schober, P., Boer, C. and Schwarte, L. A., 2018, "Correlation coefficients: appropriate use and interpretation", *Anesth Analg*, **126**, 1763-1768.
- Vu, T. M., Raghavan, S. V., Liang, S. Y. and Mishra, A. K., 2017, "Uncertainties of gridded precipitation observations in characterizing Spatio-temporal drought and wetness over Vietnam", *International Journal of Climatology*, **38**, 2067-2081.
- WMO-World Meteorological Organization. Standardized Precipitation Index User Guide (M. Svoboda, M. Hayes and D. Wood). (WMO-No. 1090), Geneva, 2012.